Supplementary information for

Nature-inspired salt resistant polypyrrole-wood for highly efficient solar steam generation

Wei Huang,[a] Gaoyue Hu,[a] Cheng Tian,[a] Xiaohong Wang,[a] Jinchun Tu, [a] Yang Cao,[*a, b] Kexi Zhang[*a]

[a] *State Key Laboratory of Marine Resource Utilization in South China Sea, College of Materials and Chemical Engineering, Hainan University, Haikou 570228, P. R. China.*

[b] *Qiongtai Normal University, Haikou 571127, PR China.*

---

[*] Corresponding author. Tel: +86 898 66292367; fax: +86 898 66292367.
E-mail address: cy507@hainu.edu.cn
[*] Corresponding author. Tel: +86 898 66292367; fax: +86 898 66292367.
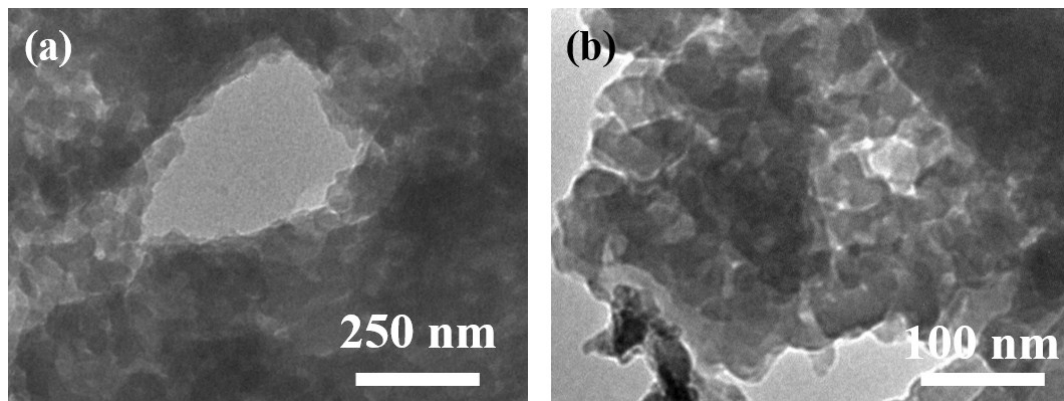*E-mail address*: zhangkexi@hainu.edu.cn

1. TEM characterization.

Figure S1. TEM images of the PPy-wood with different magnification.
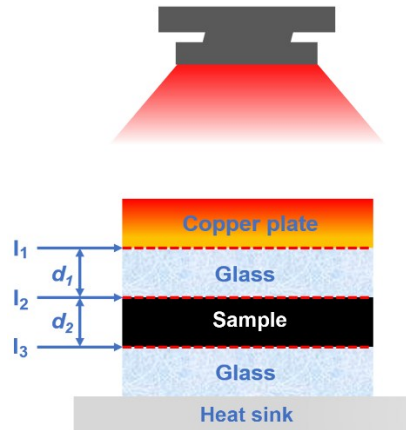
2. Thermal conductivity measurement

Figure S2. Schematic diagram of the sandwiching process showing locations for temperature measurements.

The wood sample with thickness of 3.0 mm was sandwiched between two 3 mm glasses. The sandwich structure was placed between a heating source (light source heated copper plate) and a cooling source (ice-water bath). Thermal equilibrium was achieved when the temperature variation within 10 min was less than 0.2 K. **Figure S2** shows the schematic of the sandwiching process and the locations for the temperature measurements. The temperature at the three interfaces (copper plate–top glass (I_1), top glass–wood sample (I_2), and wood sample–bottom glass (I_3)) were detected using an IR camera. During heating, the temperature gradient (dT/dx) in the vertical direction appears on the sandwich structure. The heat transfer rate (q) permeating the sandwich structure can be calculated using the Fourier equation:

$$q = -k_1 \frac{dT}{dx} = -k_1 \frac{T_2 - T_1}{d_1}$$

where k_1 is the thermal conductivity of quartz glass (1.05 W·m^{-1}·K^{-1}) (Carbon, 2017, 114: 117–124; Energy Conversion and Management, 2015, 96: 605–612.), T_1 and T_2 are the average temperatures at the interfaces I_1, and I_2, respectively, and d_1 = 3.0 mm is the thickness of the glass. After the heat transfer rate was obtained, the thermal conductivity of the wood sample (k) was calculated using:

$$k = -q \frac{d_2}{T_3 - T_2}$$

where T_3 is the average temperature at the interface I_3, and $d_2 = 3.0$ mm is the thickness of the test sample.
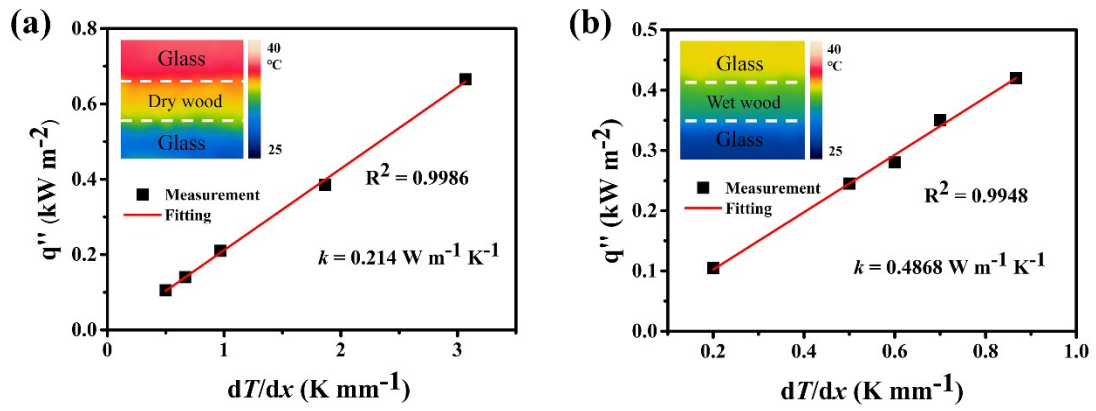

Figure S3. Thermal conductivities of the bare-wood in (a) dry and (b) wet states.

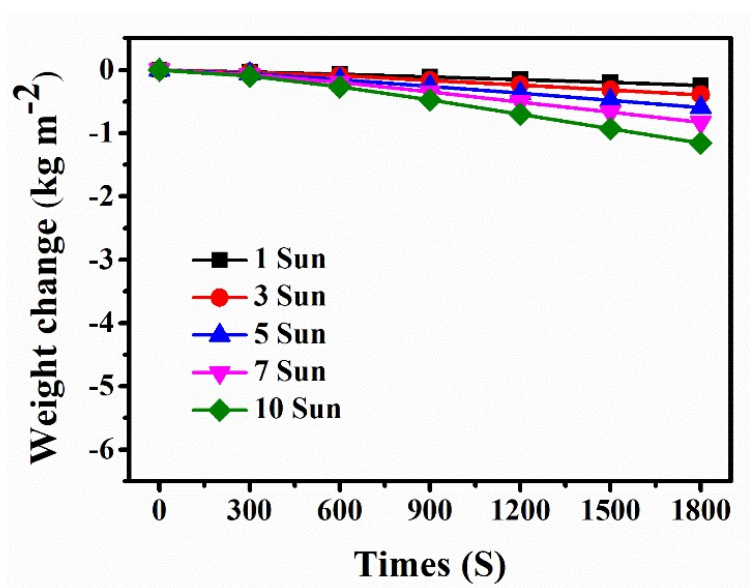**3. Weight loss for the PPy-wood at different light intensities.**

Figure S4. Weight loss for the PPy-wood at different light intensities of 1-10 Sun.

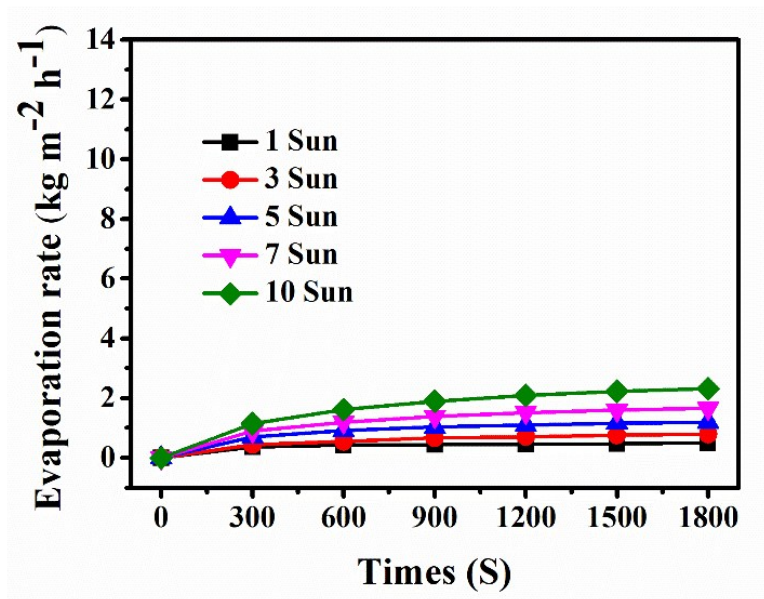**4. Solar steam generation dynamics of the pure water.**

Figure S5. Solar steam generation dynamics of the pure water at different light intensities of 1-10 Sun.
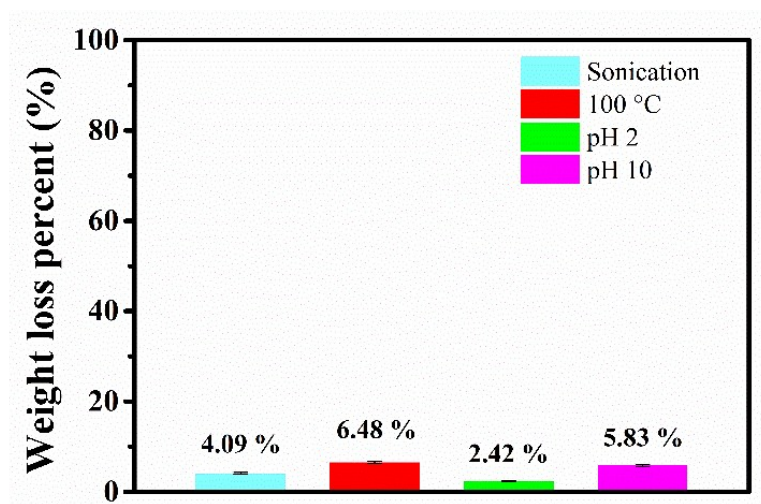
5. Stability analysis

Figure S6. Weight loss of the PPy-wood samples under different conditions.

The weight loss percent of each sample can be calculated by the following equation:

$$W_x\%=(W_{bx}-W_{ax}-W_{ox})\times100\%/W_{PPy}$$

Where x represents the treating conditions, W_x represents the weight loss under different conditions, W_a represents the dry weight before immersion, W_b represents dry weight after immersion, W_L represents average weight loss of the pure wood, W_o represents dry weight after different immersion conditions, and W_{PPy} represents the average production of the PPy particles. All the wood samples were tailed with the same size (30×30×5mm). It can be seen in **Figure S6** that the PPy-wood samples show low weight loss percentages even under extremely conditions.

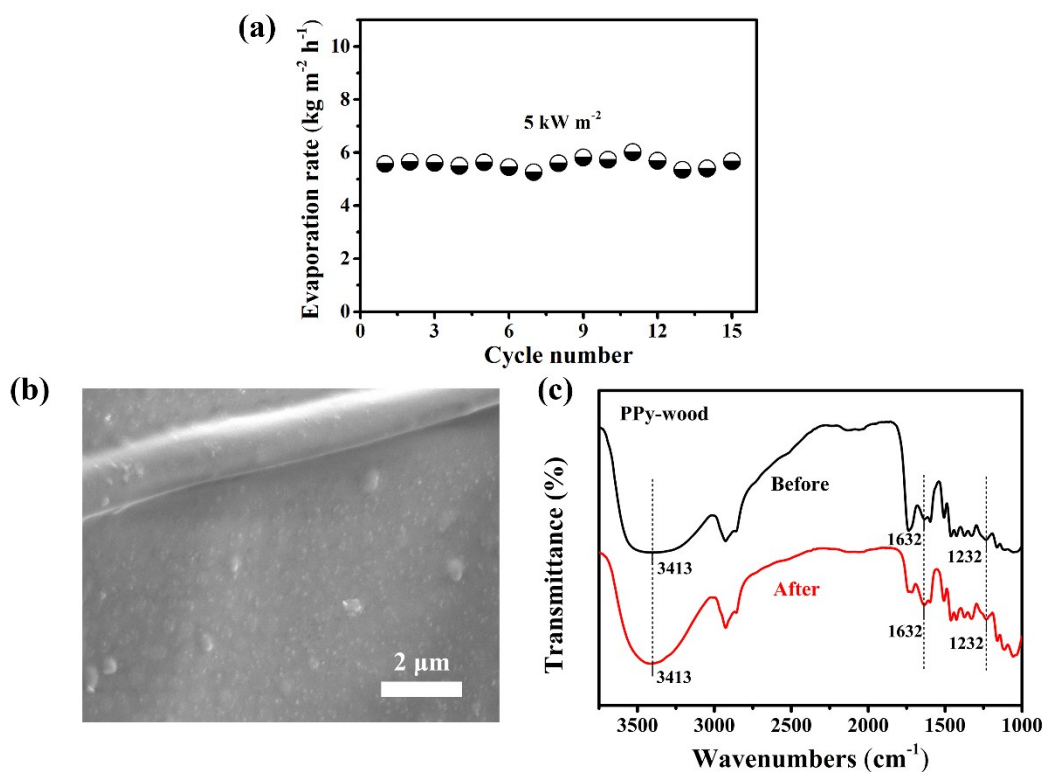**6. Cycling stability of the PPy-wood under 5 Sun illumination.**

Figure S7. (a) Cycling stability of the PPy-wood under 5 Sun illumination for 30 min over 15 cycles. (b) SEM image and (c) FTIR spectral of the PPy-wood after tests.

As shown in **Figure S7a**, even under a high illumination intensity of 5 Sun, the PPy-wood could maintain relatively stable evaporation rates for 15 cycles. After a long-time cycling test, the PPy coating still well retained on the surface of the wood matrix (**Figure S7b**). The FTIR spectral (**Figure S7c**) shows that the PPy-wood after the cycling test retained almost all of the absorption peaks before the test, indicating a good cycling stability.

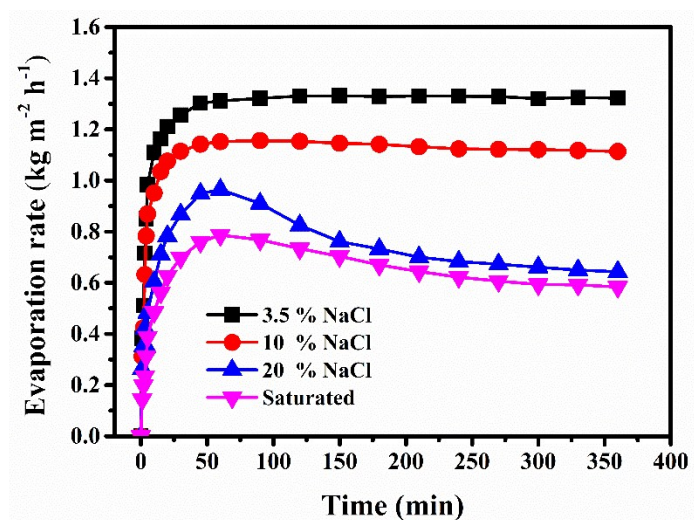**7. Time-dependent steam generation of the PPy-wood.**

Figure S8. Time-dependent steam generation of the PPy-wood under different salinities with 1 Sun illumination.

8. Solar steam generation performance comparison.

Table S1. Comparison of the evaporation rate of the water in recently reports.

Sample	Evaporation rate (kg m^{-2} h^{-1})	Conversion efficiency (%)	Reference
F-Wood/CNTs membrane	0.95	65 %	[1]
F-wood	1.05	72 %	[2]
GO-SA-CNT Aerogels	1.32	83 %	[3]
PPy coated SS	0.92	58 %	[4]
Ti$_2$O$_3$	1.32	83 %	[5]
Black AuNP film		77.8 %	[6]
Black Al-Ti-O membrane	1.24	77.5 %	[7]
CNT-silica	1.31	82 %	[8]
Cu$_7$S$_4$	1.23	77.1%	[9]
PPy-wood	1.33	83 %	This work

9. Estimating the cost of the PPy-wood.

Table S2. Estimating the cost of the PPy-wood.

Reagents	Price	Manufacturer
Wood	0.0008 $/cm^2	
Pyrrole	0.1400 $/mL	Aladdin
APS	0.0048 $/g	Guangzhou Chemical Reagent Factory
HCl	0.0045 $/mL	Guangzhou Chemical Reagent Factory

0.1 ml pyrrole + 0.456 g APS + 2 mL HCl + wood (9 cm^2)

= 0.1×0.1400 + 0.456×0.0048 + 2×0.0045 + 0.0008×9

= 0.0140 + 0.0022 + 0.0090 + 0.0072

= 0.0324 $/(9 cm^2)

= 36 $/m^2

Actually, for most of the solutions such as APS and HCl, it can be reused at least twice, so the given cost evaluation can be further reduced. Considering that entire preparation process is quite simple, the total cost could be very attractive compared with the noble metal and new carbon materials.

References

1. C. Chen, Y. Li, J. Song, Z. Yang, Y. Kuang, E. Hitz, C. Jia, A. Gong, F. Jiang, J. Y. Zhu, B. Yang, J. Xie and L. Hu, *Advanced Materials*, 2017, **29**, 1701756-n/a.

2. G. Xue, K. Liu, Q. Chen, P. Yang, J. Li, T. Ding, J. Duan, B. Qi and J. Zhou, *ACS Applied Materials & Interfaces*, 2017, **9**, 15052-15057.

3. X. Hu, W. Xu, L. Zhou, Y. Tan, Y. Wang, S. Zhu and J. Zhu, *Advanced Materials*, 2017, **29**, 1604031.

4. L. Zhang, B. Tang, J. Wu, R. Li and P. Wang, *Advanced Materials*, 2015, **27**, 4889-4894.

5. J. Wang, Y. Li, L. Deng, N. Wei, Y. Weng, S. Dong, D. Qi, J. Qiu, X. Chen and T. Wu, *Advanced Materials*, 2017, **29**, 1603730-n/a.

6. Y. Liu, S. Yu, R. Feng, A. Bernard, Y. Liu, Y. Zhang, H. Duan, W. Shang, P. Tao, C. Song and T. Deng, *Advanced Materials*, 2015, **27**, 2768-2774.

7. L. Yi, S. Ci, S. Luo, P. Shao, Y. Hou and Z. Wen, *Nano Energy*, 2017, **41**, 600-608.

8. Y. Wang, L. Zhang and P. Wang, *ACS Sustainable Chemistry & Engineering*, 2016, **4**, 1223-1230.

9. C. Zhang, C. Yan, Z. Xue, W. Yu, Y. Xie and T. Wang, *Small*, 2016, **12**, 5320-5328.